

Ionization Mechanisms of HBLR and Non-HBLR Seyfert 2 Galaxies

Po-Chieh Yu & Chorng-Yuan Hwang

Graduate Institute of Astronomy, National Central University, Chung-Li 32001, Taiwan

pcyu@astro.ncu.edu.tw, hwangcy@astro.ncu.edu.tw

ABSTRACT

We investigate the ionization mechanisms for hidden broad-line region (HBLR) and non-HBLR Seyfert 2 galaxies by comparing some optical emission line ratios. We note that the $[\text{N II}] \lambda 6583/\text{H}\alpha$ ratio of the non-HBLR Seyfert 2 galaxies is significantly higher than that of the HBLR Seyfert 2 galaxies while other line ratios, such as $[\text{O III}]/\text{H}\beta$ and $[\text{O I}]/\text{H}\alpha$ are similar. To probe the origin of this difference, we explore theoretical results of different ionization models, such as photoionization, starburst, and shock models. We find that none of these models can explain the high $[\text{N II}] \lambda 6583/\text{H}\alpha$ ratio of the non-HBLR Seyfert 2 galaxies with solar abundance; the high $[\text{N II}] \lambda 6583/\text{H}\alpha$ must be reproduced from enhanced nitrogen abundance. Since nitrogen overabundance can be achieved from the dredge-up of red supergiants in the post-main-sequence stage, we suggest that the observed nitrogen overabundance of the non-HBLR Seyfert 2 might be caused by stellar evolution, and there could be an evolutionary connection between the HBLR and non-HBLR Seyfert 2 galaxies.

Subject headings: galaxies: active – galaxies: nuclei – galaxies: Seyfert

1. INTRODUCTION

Seyfert galaxies are classified as radio-quiet active galactic nuclei (AGNs) and further divided into two subtypes, Seyfert 1 and Seyfert 2, according to their different optical line widths. Base on the orientation-based unification model (Antonucci & Miller 1985; Antonucci 1993), Seyfert 2 galaxies are considered to be the same objects as Seyfert 1 galaxies but viewed from a different direction. The detection of polarized broad permitted emission lines in several Seyfert 2 galaxies further supported this unification model (Tran 1995; Young et al. 1996; Heisler et al. 1997; Moran et al. 2000). However, previous studies showed that only about 40% - 45% of Seyfert 2 galaxies have polarized hidden broad

line regions (HBLR) (Heisler et al. 1997; Gu & Huang 2002). Spectropolarimetric studies of Seyfert 2 galaxies showed that the HBLR Seyfert 2 galaxies have higher luminosities of [O III], optical, radio and mid infrared than the non-HBLR Seyfert 2 galaxies (Gu & Huang 2002; Tran 2003). Besides, for several observational properties, such as S_{20cm}/f_{60} , f_{25}/f_{60} , and $L_{[OIII]}$, the HBLR Seyfert 2 galaxies are found to be similar to Seyfert 1 galaxies, and the non-HBLR Seyfert 2 galaxies are noted to be more like HII/starburst galaxies (Gu & Huang 2002; Deluit 2004).

It is unclear why some but not all Seyfert 2 galaxies have detectable HBLRs. Several possibilities have been proposed: (1) From the ratios of f_{25}/f_{60} , Heisler et al. (1997) suggested that the detectability of the HBLR in Seyfert 2 galaxies is related to the inclination of the torus. (2) Some evolutionary processes might be at work between the HBLR and non-HBLR Seyfert 2 galaxies (Tran 2003). (3) Zhang & Wang (2006) found that the non-HBLR Seyfert 2 galaxies and narrow line Seyfert 1 galaxies (NLS1s) have similar distribution of black hole masses, accretion rates and the ratios of f_{25}/f_{60} . They thus concluded that the non-HBLR Seyfert 2 galaxies are the counterparts of the NLS1s at edge-on orientation. (4) The non-HBLR Seyfert 2 galaxies could be mainly powered by nuclear starbursts rather than accretion onto the central black hole (Yu & Hwang 2005). (5) From X-ray data, Shu et al. (2007) indicated that the nuclear activity and obscuration might play an important role in the visibility of polarized broad lines. (6) Elitzur & Ho (2009) showed that the broad line regions might disappear at low luminosities in advection-dominated accretion models. (7) Tran et al. (2011) suggested that some Seyfert 2 galaxies could intrinsically lack broad line regions. (8) Some Seyfert 2 galaxies might be deficient in scattering material.

Emission lines have long been used to distinguish the origin of active galaxies. For example, optical emission lines of Seyfert 2 galaxies, such as [O III], [O I], [N II], and [S II], are usually more stronger than those of HII/starburst galaxies relative to the recombination lines. For Seyfert galaxies, photoionization from a power-law continuum, presumedly from the central AGN, is proposed to be responsible for the ionization mechanisms and is generally successful in reproducing observed optical lines (Veilleux & Osterbrock 1987). If the non-HBLR Seyfert 2 galaxies were powered by nuclear starburst activities, one important question is how the narrow line regions (NLRs) of the non-HBLR Seyfert 2 galaxies are ionized. However, we note that Terlevich et al. (1992) have showed that most of line ratios of the Seyfert 2 galaxies could be reproduced by starburst models. Besides, a photoionization model with power-law continuum might fail to reproduce all observed properties in some cases. For example, observations of [O III] suggested that the electron temperature could be up to $\sim 22,000$ K (Tadhunter et al. 1989) while the photoionization model could only give a lower one ($\sim 11,000$ K). Therefore, some other physical processes, such as shock-heating and starburst, might also play a significant role even in a photoionization dominated model

(Kraemer et al. 1998). These results suggest that we need to consider different ionization mechanisms when we investigate the origin of the ionization for Seyfert 2 galaxies.

In this paper, we investigate and compare possible ionization mechanisms of the NLRs for the HBLR and non-HBLR Seyfert 2 galaxies by considering photoionization, shock-wave heating, and starburst models. We calculate line ratios of the photoionization model with the Cloudy program of version 08.00, last described by Ferland et al. (1998). The shock models are obtained from the library calculated by Allen et al. (2008) with the MAPPING III code, and the starburst models are obtained from Kewley et al. (2001).

2. LINE RATIOS OF HBLR AND NON-HBLR SEYFERT 2 GALAXIES

2.1. Diagnostic Diagrams

Active galaxies, such as starburst and Seyfert 2, show narrow emission lines in their spectra. The line ratio $[\text{O III}] \lambda 5007 / \text{H}\beta \geq 3$ was found to be a good criterion to separate Seyfert 2 and starburst or H II-like galaxies (Shuder & Osterbrock 1981). However, some starburst galaxies were also found to have $[\text{O III}] \lambda 5007 / \text{H}\beta \geq 3$ (Osterbrock & De Robertis 1985). Other line ratios, such as $[\text{N II}] \lambda 6583 / \text{H}\alpha$, $[\text{O I}] \lambda 6300 / \text{H}\alpha$ and $[\text{S II}] \lambda \lambda 6716, 6731 / \text{H}\alpha$, are also needed to separate the starburst and Seyfert 2 galaxies (Baldwin et al. 1981; Veilleux & Osterbrock 1987). In Figure 1, we show the diagnostic diagram of these line ratios; the data of the HBLR and non-HBLR Seyfert 2 galaxies are collected from literatures and listed in Table 1. The data of H II-like galaxies and LINERs are adopted from Ho et al. (1997).

Beside the well-known separation between the starburst and Seyfert 2 galaxies, we note that the distribution of the non-HBLR Seyfert 2 is very different from that of the HBLR ones. The difference is mainly caused by the different line ratio of $[\text{N II}] \lambda 6583 / \text{H}\alpha$. Both Kolmogorov-Smirnov test ($P = 99.7\%$) and Student's T-test ($P = 99.9\%$) show that the $[\text{N II}] \lambda 6583 / \text{H}\alpha$ distribution of the HBLR and non-HBLR Seyfert 2 galaxies are significantly different. This indicates that the HBLR and non-HBLR Seyfert 2 galaxies have different physical conditions. In order to understand the physical properties of these Seyfert 2 galaxies, we compare the observed data with different ionization mechanisms in the following.

2.2. Models

Seyfert galaxies are usually considered to be photoionized by central AGNs. The ionization source is suggested to be a power-law continuum (Koski 1978). In order to compare

with the observed data, we use the Cloudy program to produce the line ratios. The Cloudy package is designed to simulate photoionization of clouds with different incident continuum. We assume that the incident ionizing continuum is a power law with an index $p = 1.4$ and the distance from the cloud to the central continuum is set to be 100 pc. The derived ionization parameter Γ varies from $10^{-1.5}$ to $10^{-3.5}$ and the hydrogen density n_H varies from 10^2 to 10^5 cm^{-3} .

Figure 2 shows the results of Cloudy models with different nitrogen abundances. Figure 2a shows that the relative emission between [O III] and [O I] is not very sensitive to the nitrogen abundance as expected. Figure 2b indicates that the high [N II] $\lambda 6583/\text{H}\alpha$ ratio of the non-HBLR Seyfert 2 galaxies can be reproduced by increasing the nitrogen abundance to five times solar abundance ($5N_\odot$). We note that if we simply increase all metal abundance, the [O III] emission would also increase as well and would not reproduce the observed [N II]/[O III] ratio. This result suggests that the non-HBLR Seyfert 2 galaxies might have higher N/O relative abundance than the HBLR Seyfert 2 galaxies. However, as shown in Figure 2c, the [S II] emission can not be reproduced with both (N_\odot) and $5N_\odot$ abundance.

To investigate the origin of the [S II] emission, we compare the emission of [N II] with that of [S II] in Figure 3. There is a significant correlation between [N II] $\lambda 6583/\text{H}\alpha$ and [S II] $\lambda\lambda 6716, 6731/\text{H}\alpha$ for both HBLR and non-HBLR seyfert 2 galaxies as shown in Figure 3. This indicates that the emission of both [N II] and [S II] must have the same origin. We also note that the correlations might have different slopes for both kinds of galaxies; the non-HBLR Seyfert 2 galaxies seems to have a slightly steeper slope than that of the HBLR Seyfert 2 galaxies. Furthermore, the photoionization model is difficult to explain the high [N II]. This suggests that some other mechanisms might be operative for producing the observed [S II] and [N II] emission.

One other possible excitation mechanism for the NLRs of Seyfert 2 galaxies is shock-wave heating. Allen et al. (2008) has presented a library of radiative shock models calculated using the MAPPINGS III code. The parameters in the library have broad ranges with the pre-shock density n from 0.01 to 1000 cm^{-3} , the shock velocity v from 100 to 1000 km s^{-1} , the pre-shock magnetic fields B from 10^{-10} to 10^{-4} G , and the magnetic parameter $B/n^{1/2}$ from 10^{-4} to $100 \mu\text{G cm}^{3/2}$. The library of MAPPINGS III code is available in the internet.¹ We compare the observed line ratios with the results from the library.

The shock model with the standard solar abundance can reproduce the distribution of the [O I] and [S II] emission. On the other hand, the [N II] emission of the non-HBLR Seyfert 2 galaxies can be reproduced only by increasing metal content to two times solar

¹<http://www.ifa.hawaii.edu/~kewley/Mappings/index.html>

abundance in the shock models. This result further suggests that the nitrogen abundance of the non-HBLR Seyfert 2 galaxies are higher than that of the HBLR ones. However, it is noted that the shock models can not produce enough [O III] emission. By adding ionized pre-shock gas in the shock models (Allen et al. 2008) might be able to produce high enough [O III] emission but would fail to produce the observed [N II] emission. These results show that shock models are unable to reproduce these observed line ratios simultaneously.

Another possible ionization mechanism is starburst. A large library of starburst models has been presented by Kewley et al. (2001). However, as shown in Figure 1, only three sources lie on the extreme starburst region. It is obvious that the [N II] and [O III] line emission of the non-HBLR Seyfert 2 galaxies can not be reproduced by the starburst models. Furthermore, if the [N II] emission is from starburst region, high [O II] emission would be expected. However, the averaged [O II]/[O III] ratio is 0.23 ± 0.16 and 0.26 ± 0.09 for the HBLR and non-HBLR Seyfert 2 galaxies (Gu et al. 2006), indicating the contribution from star formation is similar for the HBLR and non-HBLR Seyfert 2 galaxies. Besides, Kewley et al. (2001) indicated that the contribution from supernovae to the starburst models is $\ll 20\%$ and can be neglected. Therefore, the starburst models would hardly explain these line ratios even including supernova contribution.

Based on these results, all the line ratios can not be reproduced by one single model. This might not be unreasonable since NLRs could be composed of clouds with different ionization conditions. For example, the [O III] emission could come from highly ionized regions that powered by AGNs while [N II] emission come from lower ionized regions. One possibility to explain the observed line ratios is a composite model of an AGN continuum and starburst and/or shock. However, the [N II]/H α line ratios produced by these three single models with solar abundance are all much less than observations, so any combination of these three models can not produce enough [N II] emission for the non-HBLR Seyfert 2 galaxies. This result suggests that the high [N II]/H α ratios must be due to over abundance of nitrogen in the non-HBLR Seyfert 2 galaxies.

3. DISCUSSION

It is not unusual for Seyfert 2 galaxies to show enhanced nitrogen abundance. Previous studies showed that the nitrogen abundance of Seyfert 2 galaxies can reach to 3.5–5 solar abundance (Storchi-Bergmann & Pastoriza 1990). Our results further show that the non-HBLR Seyfert 2 galaxies have higher nitrogen abundance than the HBLR Seyfert 2 galaxies. Comparing these results, we suggest that the high nitrogen abundance of the Seyfert 2 galaxies in early studies might be mainly caused by the non-HBLR Seyfert 2 galaxies.

The difference between the HBLR and non-HBLR might be caused by their stellar evolution. Based on evolutionary models of starburst activities, Matteucci & Padovani (1993) showed that the N/O relative abundance reaches a maximum value at about 3×10^8 years. The nitrogen could be dredged up from red supergiants in the post-main-sequence stage, and this would result in the nitrogen overabundance. Therefore, the super-solar nitrogen abundance of the non-HBLR Seyfert 2 galaxies may imply that the starburst activities in the non-HBLR Seyfer 2 galaxies are in the post-main-sequence stage.

The high abundance of the non-HBLR Seyfert 2 galaxies implies that there could be an evolutionary connection between the non-HBLR and HBLR Seyfert 2 galaxies. AGNs have been suggested to be related to circumnuclear star formation. Accreted gas is transported to the central regions to fuel the AGNs; the transported gas accumulates around the nucleus and might also trigger star formation. The super-solar abundance suggests that the non-HBLR Seyfert 2 galaxies are in older stages of stellar evolution than the HBLR Seyfert 2 galaxies. This would also imply that the gas around the nucleus of the non-HBLR Seyfert 2 galaxies might have diminished, which would cause low accretion rates for the non-HBLR Seyfert 2 galaxies. This is consistent with the results found by Bian & Gu (2007), which showed that the accretion rates of non-HBLR Seyfert 2 galaxies are lower than those of HBLR Seyfert 2 galaxies. When the accretion rate is below some thresholds, the broad line regions could disappear (Nicastro et al. 2003); therefore, no polarized broad lines are observed in the non-HBLR Seyfert 2 galaxies.

4. SUMMARY

We investigate the ionization mechanisms of the HBLR and non-HBLR Seyfert 2 galaxies by comparing the photoionization, shock, and starburst results with observations. A possible explanation for all observed emission might require combination of different models; for example, the [O III] emission could come from highly ionized regions that powered by AGNs while [N II] emission come from lower ionized regions by starburst or shock waves. However, our results show that the non-HBLR Seyfert 2 galaxies must have higher N/O relative abundance than the HBLR Seyfert 2 galaxies. The high N/O relative abundance could originate from stellar evolution and imply an evolutionary connection between the HBLR and non-HBLR Seyfert 2 galaxies. As a HBLR Seyfert 2 galaxy evolves, the gas around the nucleus become diminished, resulting in low accretion rates and depleting the broad line regions; this evolution might transfer HBLR Seyfert 2 galaxies to non-HBLR ones.

We thank the referee for constructive comments. We are also grateful to the groups

and persons who provide the Cloudy code and the MAPPINGS III library. This work was partially supported by the National Science Council of Taiwan (grants NSC 99-2112-M-008-014-MY3 and NSC 99-2119-M-008-017). This research has made use of the NASA/IPAC Extragalactic Database (NED) which is operated by the Jet Propulsion Laboratory, California Institute of Technology, under contract with the National Aeronautics and Space Administration.

REFERENCES

- Allen, M. G., & Groves, B. A., & Dopita, M. A., & Sutherland, R. S., & Kewley, L. J. 2008, *ApJS*, 178, 20
- Antonucci, R. R. J., & Miller, J. S. 1985, *ApJ*, 297, 621
- Antonucci, R. R. J. 1993, *ARA&A*, 31, 473
- Baldwin, J. A., Phillips, M. M., & Terlevich, R. 1981, *Pub. A. S. P.*, 93, 5
- Bian, W., & Gu, Q. 2007, *ApJ*, 657, 159
- de Grijp, M. H. K., Keel, W. C., Miley, G. K., Goudfrooij, P., & Lub, J. 1992, *A&AS*, 96, 389
- Deluit, S. J. 2004, *A&A*, 415, 39
- Elitzur, E., & Ho, L. C. 2009, *ApJL*, 701, L91
- Ferland, G. J., Korista, K. T., Verner, D. A., Ferguson, J. W., Kingdon, J. B., & Verner, E. M. 1998, *PASP*, 110, 761
- Frogel, J. A., Gillett, F. C., Terndrup, D. M., & Vader, J. P. 1989, *ApJ*, 343, 672
- Gu, Q., & Huang, J. 2002, *ApJ*, 579, 205
- Gu, Q., Melnick, J., Cid Fernandes, R., Kunth, D., Terlevich, E., & Terlevich, R. 2006, *MNRAS*, 366, 480
- Heisler, C. A., Lumsden, S. L., & Bailey, J. A. 1997, *Nature*, 385, 700
- Ho, L. C., Filippenko, A. V., & Sargent, W. L. W. 1997, *ApJS*, 112, 315
- Kauffmann, G., et al. 2003, *MNRAS*, 346, 1055

- Koski, A. T. 1978, *ApJ*, 223, 56
- Kewley, L. J., Dopita, M. A., Sutherland, R. S., Heisler, C. A., & Trevena, J. 2001, *ApJ*, 556, 121
- Kewley, L. J., Heisler, C. A., & Dopita, M. A. 2001, *ApJS*, 132, 37
- Kewley, L. J., Groves, G., Kauffmann, G., & Heckman, T. 2006, *MNRAS*, 372, 961
- Kraemer, S. B., Ruiz, J. R., & Crenshaw, D. M. 1998, *ApJ*, 508, 232
- Matteucci, F., & Padovani, P., 1993, *ApJ*, 419, 485
- Moran, E. C., Barth, A. J., Kay, L. E., & Filippenko, A. V. 2000, *ApJ*, 540, L73
- Nicastro, F., Martocchia, A., & Matt, G. 2003, *ApJ*, 589, L13
- Osterbrock, D. E., & De Robertis, M. M. 1985, *Pub. A. S. P.*, 97, 1129
- Osterbrock, D. E., & Martel A. 1993, *ApJ*, 414, 552
- Pérez, E., Manchado, A., Garcia-Lario, P., & Pottasch, S. R. 1989, *A&A*, 227, 407
- Shu, X. W., Wang, J. X., Jiang, P., Fan, L. L., & Wang, T. G. 2007, *ApJ*, 657, 167
- Shuder, J. M., & Osterbrock, D. E. 1981, *ApJ*, 250, 55
- Storchi-Bergmann, T., & Pastoriza, M. G. 1990, *PASP*, 102, 1359
- Tadhunter, C. N., Robinson, A., & Morganti, R. 1989, in *Extranuclear Activity in Galaxies*, ed. E. J. A. Meurs & R. A. E. Fosbury (Garching:ESO), 293
- Terlevich, R., Melnick, J., Masegosa, J., Moles, M., & Copetti, M. V. F. 1991, *A&AS*, 91, 285
- Terlevich, R., Tenorio-Tagle, G., & Melnick, J. 1992, *MNRAS*, 255, 713
- Tran, H. D. 1995, *ApJ*, 440, 565
- Tran, H. D. 2003, *ApJ*, 583, 632
- Tran, H. D., Lyke, J. E., & Mader, J. A. 2011, *ApJ*, 726, L21
- Vaceli, M. S., Viegas, S. M., Gruenwald, R., & de Souza, R. E. 1997, *AJ*, 114, 1345
- Vader, J. P., Frogel, J. A., Terndrup, D. M., & Heisler C. A. 1993, *AJ*, 106, 1743

Veilleux, S., & Osterbrock, D. E. 1987, *ApJS*, 63, 295

Veilleux, S., Kim, D. -C., Sanders, D. B., Mazzarella, J. M., & Soifer, B. T. 1995, *ApJS*, 98, 171

Young, S., Hough, J. H., Efstathiou, A., Wills, B. J., Axon, D. J., Bailey, J. A., & Ward, M. J. 1996a, *MNRAS*, 279, L72

Young, S., Hough, J. H., Efstathiou, A., Wills, B. J., Bailey, J. A., Ward, M. J. & Axon, D. J. 1996b, *MNRAS*, 281, 1206

Yu, P.- C., & Hwang, C.- Y. 2005, *ApJ*, 631, 720

Zhang, E., & Wang, J. 2006, *ApJ*, 653, 137

Table 1. Line Ratios of HBLR and Non-HBLR Seyfert 2 Galaxies

Name	[O III] λ 5007/H β	[O I] λ 6300/H α	[N II] λ 6583/H α	[S II] λ 6720/H α	Ref.
HBLR Seyfert 2 Galaxies					
IC 3639	0.98	-1.10	-0.11	-0.31	(1)
IC 5063	0.99	-0.93	-0.20	-0.28	(1)
IRAS 01475-0740	0.72	...	-0.31	...	(2)
IRAS 02581-1136	1.19	...	-0.09	...	(2)
IRAS 04385-0828	0.33	...	-0.19	...	(2)
IRAS 05189-2524	1.53	-1.12	0.03	-0.72	(3)
IRAS 11058-1131	0.96	-1.28	-0.42	-0.59	(4)
IRAS 15480-0344	1.28	-1.30	-0.18	-0.66	(4)
IRAS 18325-5926	0.66	...	-0.20	...	(1)
IRAS 20460+1925	0.78	-1.23	-0.28	-0.62	(5)
IRAS 22017+0319	0.97	...	-0.32	...	(2)
MCG 5-23-16	-0.40	-0.28	-0.11	-0.07	(6)
Mrk 1210	1.02	-0.66	-0.34	-0.73	(7)
Mrk 3	1.17	...	-0.01	...	(2)
Mrk 348	1.14	...	-0.15	...	(2)
Mrk 573	1.01	-0.96	-0.11	-0.29	(8)
NGC 1068	1.11	-1.06	-0.12	-0.62	(9)
NGC 2273	0.76	-0.92	-0.07	-0.33	(9)
NGC 424	0.66	-1.20	-0.41	-0.81	(10)
NGC 4388	1.05	-0.80	-0.24	-0.21	(9)
NGC 4507	0.88	-0.85	-0.24	-0.42	(1)
NGC 5252	0.84	-0.37	-0.06	-0.09	(8)
NGC 5347	0.95	...	-0.11	...	(2)
NGC 591	0.99	-0.87	0.05	-0.22	(6)
NGC 5929	0.57	-0.58	-0.22	-0.16	(8)
NGC 5995	1.15	-0.72	0.15	...	(1)
NGC 7212	1.07	-0.78	-0.14	-0.34	(1)
NGC 7674	1.03	-1.30	-0.01	-0.49	(1)
NGC 7682	0.97	-0.58	0.01	-0.15	(8)
NGC 788	1.30	-0.37	-0.10	-0.19	(10)

Table 1—Continued

Name	[O III] $\lambda 5007/H\beta$	[O I] $\lambda 6300/H\alpha$	[N II] $\lambda 6583/H\alpha$	[S II] $\lambda 6720/H\alpha$	Ref.
IRAS 00521-7054	0.99	-0.88	-0.03	-0.46	(11)
IRAS 23060+0505	0.97	...	-0.27	...	(2)
NGC 5506	0.88	-0.84	-0.09	-0.13	(1)
Non-HBLR Seyfert 2 Galaxies					
IRAS 00198-7926	0.50	-1.25	-0.30	-0.48	(1)
IRAS 03362-1642	0.79	...	-0.20	...	(2)
IRAS 04229-2528	0.60	...	-0.01	...	(2)
IRAS 04259-0440	0.30	-0.85	-0.11	-0.44	(1)
IRAS 08277-0242	1.15	...	0.11	...	(2)
IRAS 13452-4155	0.92	-0.78	-0.21	-0.37	(11)
IRAS 20210+1121	0.79	-0.99	-0.17	-0.50	(12)
IRAS 23128-5919	0.48	-10.00	-0.49	-0.70	(1)
Mrk 1066	0.59	-1.03	-0.06	-0.41	(6)
Mrk 334	0.23	-1.28	-0.23	-0.55	(8)
NGC 1144	0.88	-0.63	0.27	-0.08	(8)
NGC 1241	0.74	-0.14	-0.03	-0.27	(10)
NGC 1320	1.05	-0.90	-0.15	-0.38	(10)
NGC 1358	1.05	-0.59	0.30	-0.02	(9)
NGC 1386	1.57	-1.10	0.20	-0.14	(1)
NGC 1667	0.88	-0.62	0.38	-0.02	(9)
NGC 1685	0.87	...	-0.08	...	(2)
NGC 3079	0.62	-0.74	0.20	-0.07	(9)
NGC 3281	1.00	-1.03	-0.01	-0.26	(1)
NGC 3362	0.92	-0.65	0.38	-0.06	(8)
NGC 34	0.50	-0.93	0.10	-0.33	(3)
NGC 3982	1.33	-0.49	-0.06	-0.24	(9)
NGC 4501	0.73	-0.72	0.32	-0.03	(9)
NGC 5135	0.69	-1.19	-0.04	-0.45	(1)
NGC 5194	0.95	-0.80	0.46	-0.07	(9)
NGC 5256	0.62	-1.25	-0.25	-0.44	(3)
NGC 5283	0.79	-0.58	-0.06	-0.11	(8)

Table 1—Continued

Name	[O III] $\lambda 5007/H\beta$	[O I] $\lambda 6300/H\alpha$	[N II] $\lambda 6583/H\alpha$	[S II] $\lambda 6720/H\alpha$	Ref.
NGC 5643	1.11	-0.73	0.06	-0.15	(1)
NGC 5695	1.02	-0.55	0.17	0.03	(6)
NGC 6300	0.96	-0.52	0.35	-0.03	(10)
NGC 7172	1.00	-0.78	0.00	0.01	(10)
NGC 7582	-0.20	-1.68	-0.50	-0.62	(1)
IRAS 19254-7245	0.72	-0.86	0.06	-0.14	(1)

Note. — Column 2 - Column 5: Line ratio presented in logarithm. Column 6: Reference number - (1)Kewley et al. (2001); (2)de Grijp et al. (1992); (3)Veilleux et al. (1995); (4)Osterbrock & De Robertis (1985); (5)Frogel et al. (1989); (6)Veilleux & Osterbrock (1987); (7)Terlevich et al. (1991); (8)Osterbrock & Martel (1993); (9)Ho et al. (1997); (10)Vaceli et al. (1997); (11)Vader et al. (1993); (12)Pérez et al. (1989).

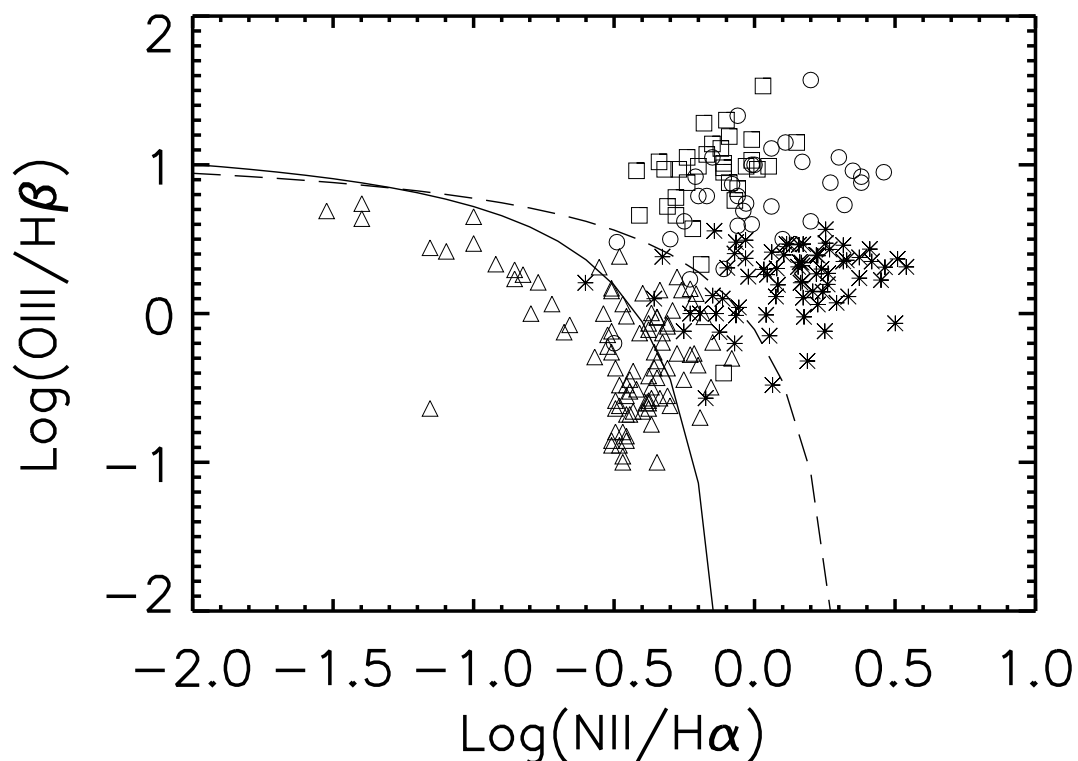


Fig. 1.— Diagnostic diagrams of [N II] and [O III] line ratios. The HBLR Seyfert 2 galaxies are shown as squares, the non-HBLR Seyfert 2 as open circles, HII like as triangles and LINER as asterisks. The solid curve represents the dividing line of star forming galaxies from Seyfert-HII composite sources (Kauffmann et al. 2003); and the dashed line represents the boundary of extreme starburst with super-solar abundance (Kewley et al. 2006).

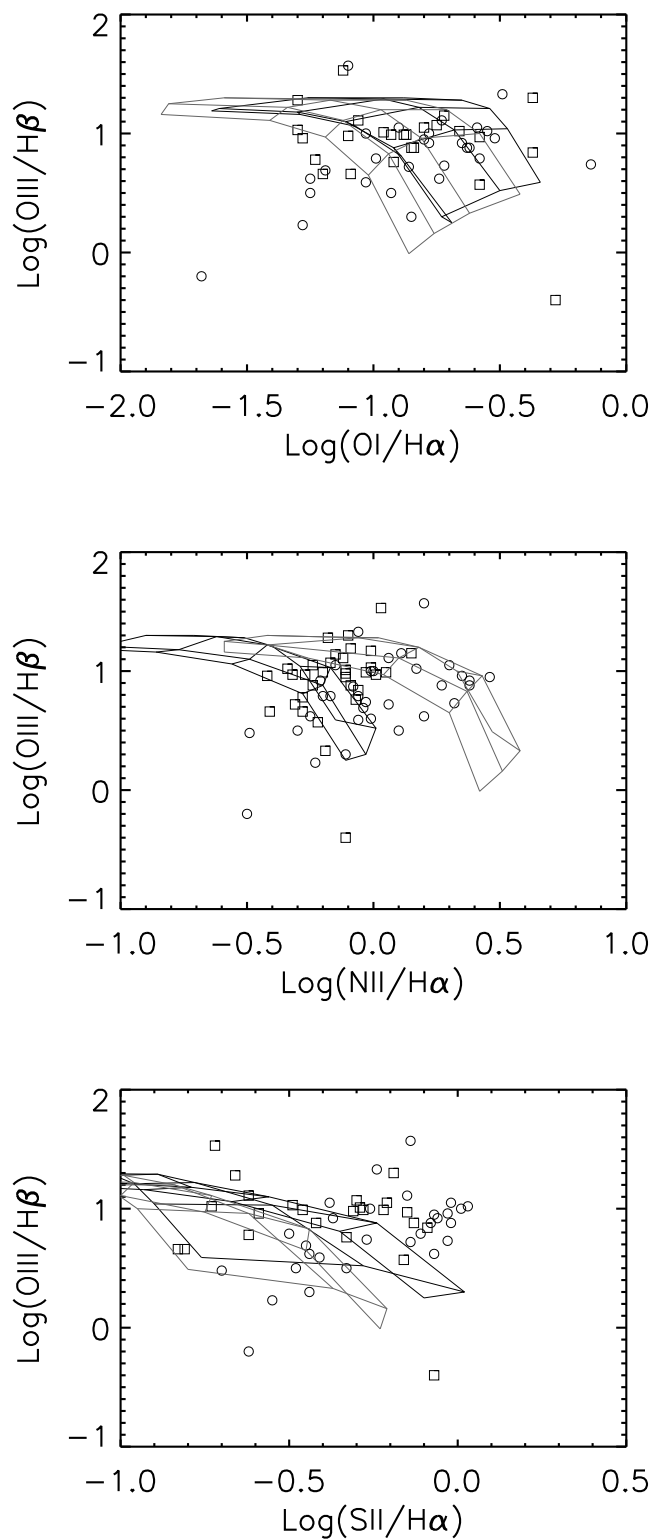


Fig. 2.— Results of photoionization models. Symbols are the same as those of Figure 1. The results with the standard solar abundance of nitrogen (N_{\odot}) are shown in black curves, and those with five times solar abundance of nitrogen ($5N_{\odot}$) are shown in grey. The ionization parameter Γ varies from $10^{-1.5}$ to $10^{-3.5}$ (upper-left to lower-right for each model), and the

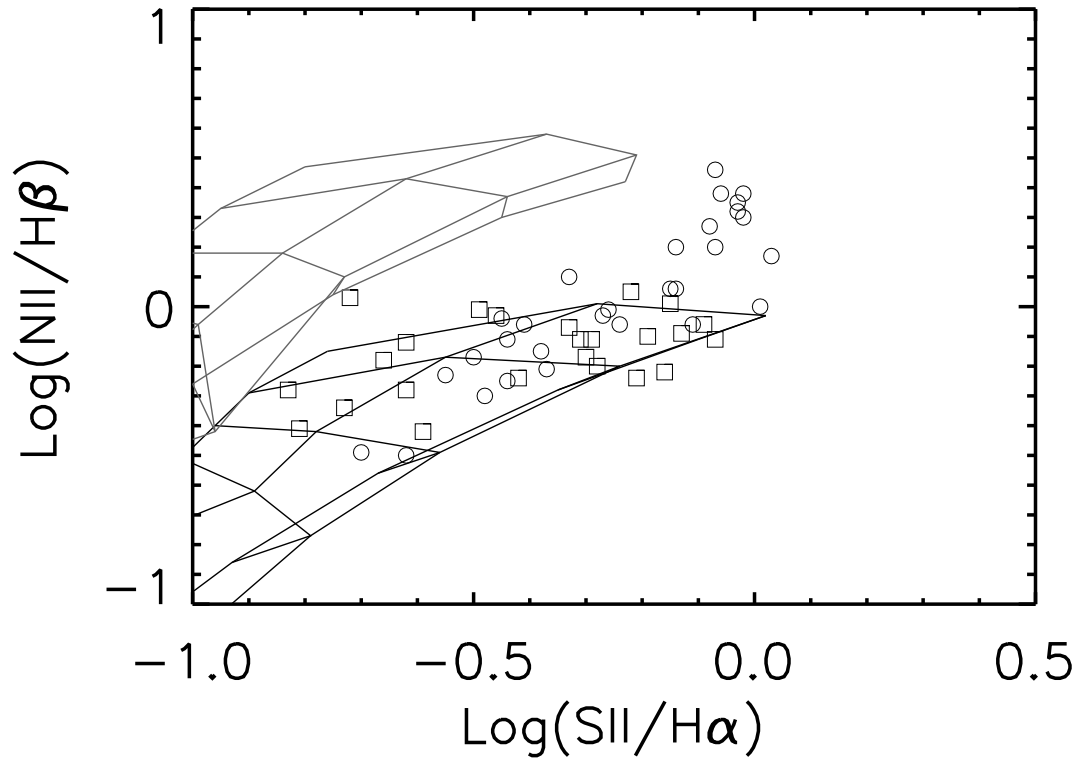


Fig. 3.— Correlation between the [N II] and [S II] emission. The results of photoionization models are also plotted in the diagram for comparison. Symbols are the same as those of Figure 1. The ionization parameter Γ varies from $10^{-1.5}$ to $10^{-3.5}$ (lower-left to upper-right for each model), and the density n_H varies from 10^2 to 10^5 (left to right for each model).